Langmuir

Article

pubs.acs.org/Langmuir

Poly(L-lysine) Interfaces via Dual Click Reactions on Surface-Bound Custom-Designed Dithiol Adsorbates

Amin Shakiba, Andrew C. Jamison, and T. Randall Lee*

Departments of Chemistry and Chemical Engineering and the Texas Center for Superconductivity, University of Houston, Houston, Texas 77204-5003, United States

Supporting Information

ABSTRACT: Surfaces modified with poly(L-lysine) can be used to immobilize selected biomolecules electrostatically. This report describes the preparation of a set of self-assembled monolayers (SAMs) from three different azide-terminated adsorbates as platforms for performing controlled surface attachments and as a means of determining the parameters that afford stable poly(L-lysine)-modified SAM surfaces having controlled packing densities. A maleimide-terminated alkyne linker was "clicked" to the azide-terminated surfaces via a copper-catalyzed cycloaddition reaction to produce the attachment sites for the polypeptides. A thiol−Michael addition was then used to immobilize cysteine-terminated poly(L-lysine) moieties on the gold surface, avoiding adsorbate self-reactions with this two-step procedure. Each step in this process was analyzed by ellipsometry, X-ray photoelectron spectroscopy, polarization modulation infrared reflection−absorption spectroscopy, and contact angle goniometry to determine which adsorbate structure most effectively produced the targeted polypeptide interface. Additionally, a series of mixed SAMs using an azidoalkanethiol in combination with a normal alkanethiol having an equivalent alkyl chain were prepared to provide data to determine how dilution of the azide reactive site on the SAM surface influences the initial click reaction. Overall, the collected data demonstrate the advantages of an appropriately designed bidentate absorbate and its potential to form effective platforms for biomolecule surface attachment via click reactions.

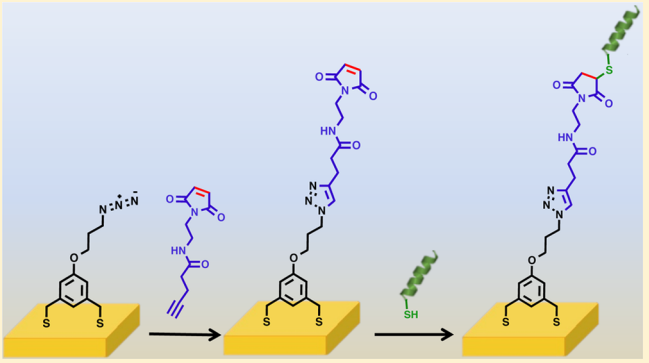

INTRODUCTION

Thin films prepared for molecular immobilization on solid supports can augment surfaces to give rise to a variety of properties in a broad array of applications such as biosensors,[1] biochips,[2] and antifouling interfaces.[3] Coating a metal surface with a self-assembled monolayer (SAM) provides one means of preparing such thin films. Because these monolayers are no thicker than a single molecule, SAMs can be used to expose an ordered array of chain termini at the interface to dictate a specific interfacial property. Additionally, if the adsorbates used to form these films are terminated with a functional group, this array of reactive sites can act as a suitable platform to attach other compounds onto the surface in a controlled orientation.[4−7] Therefore, controlled surface modification becomes a key aspect in the design of a functionalized interface for specific applications. For instance, SAMs with exposed amine, carboxylic acid, alkene, or alcohol moieties[8,9] have been used to provide a robust attachment of biomolecules such as oligonucleotides[10] and polypeptides[11] onto solid surfaces. A specific example would be the work of Chen et al., who studied the immobilization and orientation of biomolecules on surfaces.[12] This research team used functionalized interfaces to immobilize enzymes[12] and peptides[13] by either physisorption or chemisorption. A key aspect of these investigations was the development of an understanding that the formation of well-ordered thin films that present an appropriately oriented interface of biomolecules on a surface can increase the performance and sensitivity of such biomolecules in biochip and biosensor applications.

One facile route to preparing well-ordered SAMs is by exploiting the affinity of thiols toward gold. Thiolate SAMs can be prepared on a gold substrate under ambient conditions without the need for a clean-room environment. This well-known system affords a highly oriented monolayer of adsorbates that can present an array of terminal functional groups at the interface, priming the surface for further attachments. To control the attachment of new molecules such as bulky biomolecules, mixed alkanethiolate SAMs are frequently used.[14,15] These SAMs can be designed to avoid a high packing density for the adsorbates carrying the binding site—an interfacial arrangement that can hinder the efficient binding of biomolecules on a surface. Additionally, by controlling the number of bonding sites on the surface, one can structure the SAM to reduce the occurrence of random

Received: March 8, 2015
Revised: May 6, 2015
Published: May 11, 2015

DOI: 10.1021/acs.langmuir.5b00877
Langmuir 2015, 31, 6154−6163

surface orientation of the biomolecules, which can lead to an undesirably low density of the targeted surface-exposed molecule.[16]

In the present study, we designed two short-chained dithiol adsorbates having an azide functionality attached to a central aromatic ring, together with an azide-terminated alkanethiol of comparable chain length, and produced a set of azide-terminated monolayers on gold surfaces. These adsorbate structures are shown in Figure 1. Dual "click" reactions were

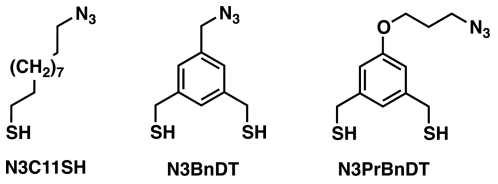

Figure 1. Structures of the azide-terminated adsorbates.

used to perform the two-step attachment of a poly(L-lysine) compound to these monolayers. The first step involved functionalization of the surface with a maleimide group and was accomplished by a Cu-catalyzed azide–alkyne cycloaddition (CuAAC) reaction to attach the alkyne-terminated maleimide linker by [3 + 2] cycloaddition. This reaction is highly regioselective and can be performed in high yield.[17,18] Notably, this approach to assembling an array of reactive bonding sites avoids possible self-reactions associated with a single composite maleimide-terminated adsorbate. The second step involved a thiol–Michael addition of the cysteine-terminated poly(L-lysine) to the maleimide and was conducted under ambient conditions;[19] this latter reaction has been used in a wide variety of materials/biomaterials applications.[2,15,20]

The use of a short-chained dithiol platform for producing a polypeptide interface offers at least three advantages when compared to related approaches involving the physisorption of peptides:[5,21] (1) a reliable site for covalent attachment of peptide molecules, (2) a highly stable monolayer on the surface,[22,23] and (3) circumvention of problems that are encountered when using adsorbates having long alkyl chains (e.g., disarray in the resulting peptide films). Further, the minor differences in structure between the two dithiol adsorbates provide an opportunity to assess the value of the added conformational mobility afforded by a limited increase in the length of the alkyl spacer extending from the rigid aromatic ring. Both the presence of the alkyl spacer and of the oxygen on the ring are expected to influence film formation and adsorbate ordering in the monolayer.

As a control, we used 11-azidoundecane-1-thiol (**N3C11SH**) as a model monodentate adsorbate to provide a basis for studying the efficiency of the click chemistry attachment of the maleimide linker. We compared the results obtained from **N3C11SH** to those obtained from the two custom-designed bidentate dithiols prepared for this study: (5-(azidomethyl)-1,3-phenylene)dimethanethiol (**N3BnDT**) and (5-(3-azidopropoxy)-1,3-phenylene)dimethanethiol (**N3PrBnDT**). All three adsorbates were used to form SAMs on evaporated "flat" gold surfaces to expose azide groups for the click reactions.

Specifically, our study compares monolayer thin films derived from **N3C11SH**, **N3BnDT**, and **N3PrBnDT** to those formed from undecanethiol (**C11SH**) and octadecanethiol (**C18SH**), which are well-characterized reference systems for determining the effectiveness of our new adsorbates for forming SAMs on gold substrates. We used ellipsometry, X-ray photoelectron spectroscopy (XPS), polarization modulation infrared reflection–absorption spectroscopy (PM-IRRAS), and contact angle goniometry to demonstrate the formation of monolayer films and to compare the conformational order of the SAMs formed from each adsorbate. Additionally, data collected after each click reaction were used to verify the completion of those reactions and to show ultimately the attachment of poly(L-lysine). This flexible platform provides a convenient strategy for immobilizing biomolecules and cells on gold surfaces for further investigation.

EXPERIMENTAL SECTION

All experimental details regarding the materials, procedures, and instruments are provided in the Supporting Information.

RESULTS AND DISCUSSION

Azide-Functionalized Self-Assembled Monolayers. *Formation of the Initial Thin Films.* The formation of SAMs from **N3C11SH**, **N3BnDT**, and **N3PrBnDT** was probed using a variety of solvents as adsorption media. The quality of the resulting SAMs was evaluated by measuring film thicknesses by ellipsometry and by determining the efficiency of the formation of sulfur–gold bonds using XPS (see Table S1 and Figure S1 in the Supporting Information). Comparisons of the ellipsometric thicknesses and XPS data revealed that the films derived from the aromatic dithiol adsorbates exhibited the most complete monolayer formation in DMSO; therefore, all experiments were conducted using DMSO to form the azide-terminated SAMs.

Analysis by Ellipsometry. Ellipsometric thickness measurements provide useful information about self-assembled monolayers, revealing whether a film is well-packed and fully developed by comparison to calculated estimates based upon molecular structure or experimental data in the literature. The **C11SH** and **C18SH** reference SAMs were developed in ethanol—a solvent that has consistently produced well-packed normal alkanethiolate SAMs, yielding elipsometric thickness measurements of 13 and 23 Å, respectively. These values fall in line with those reported previously, indicating that our evaporated gold substrates are of sufficient quality to produce well-packed thin films.[24]

Additionally, we sought to use thickness measurements acquired after each step in the syntheses of the poly(L-lysine)-terminated films to determine the effectiveness of our click reactions during each step of the film growth for the three adsorbates (*vide infra*). For our series of azide-terminated SAMs, the initial film thickness of the **N3C11SH** SAM was 12 Å, which is ∼3 Å lower than our calculated value using a procedure from the literature.[25] Also, the thicknesses of SAMs derived from the two bidentate adsorbates, **N3BnDT** and **N3PrBnDT**, were 10 and 11 Å, respectively. For these SAMs, the estimated molecular height is 9 and 12 Å, respectively,[26] which is consistent with the measured thickness considering an experimental uncertainty of no more than ±2 Å.

Analysis by XPS. XPS provides important information regarding the elemental content of a monolayer film, in addition to the character of the chemical bonds to the surface.[27] The XPS spectra for the key elements used for analyzing each of our initial SAMs are shown in Figure 2. The spectra of the binding energy (BE) region containing the Au 4f peaks for SAMs formed from each azide-terminated adsorbate are displayed in Figure 2a and contrasted to that of the reference SAM formed from **C11SH**, which produces a well-packed

DOI: 10.1021/acs.langmuir.5b00877
Langmuir 2015, 31, 6154–6163

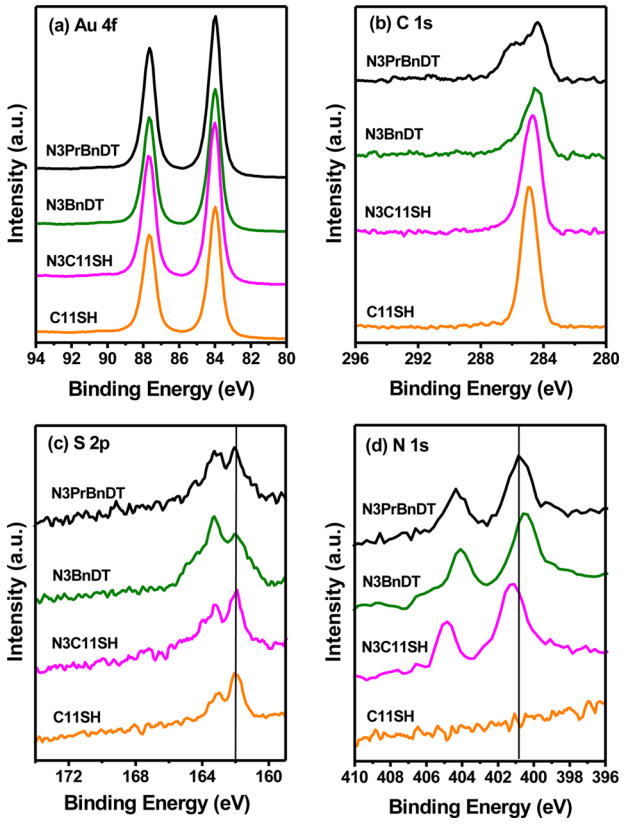

Figure 2. XPS spectra of the SAMs formed from the azide-terminated adsorbates in comparison to the **C11SH** reference SAM for the binding energy regions associated with the following peaks: (a) Au 4f, (b) C 1s, (c) S 2p (the binding energy for sulfur bound to gold is ~162 eV), and (d) N 1s (the peak at ~401 eV for **N3PrBnDT** is shifted lower than that for **N3C11SH**).

alkanethiolate monolayer having a similar film thickness. Since all four of these thin films have comparable ellipsometric thicknesses, they produce XPS spectra in the Au 4f BE region that are similar in intensity. Figure 2b shows the C 1s spectra of the SAMs formed from the azidoalkanethiolate adsorbates compared to the SAM formed from **C11SH**. The BEs for the C 1s electrons that are associated with most of the carbons involved in C−H and C−C bonds in the alkyl chain and the aromatic ring fall at ~285 eV, which is characteristic of the spectra for all of the adsorbates.[27,28] For the azidoalkanethiolate SAMs, this band can be better analyzed by deconvolution of the peaks, as provided in Figure S2 of the Supporting Information. According to literature sources, the carbon atoms adjacent to the electron-withdrawing elements (oxygen and nitrogen) exhibit BE peaks at ~286−287 eV.[27,29] For the **N3PrBnDT** SAM, a peak appears at 286.5 eV that can plausibly be assigned to the carbons bound to the ether oxygen. Additionally, a slight shoulder at 286 eV appears for the SAMs formed from **N3C11SH**, **N3BnDT**, and **N3PrBnDT**, which corresponds to the carbons adjacent to the azide group.[29]

XPS can also be used to evaluate the effectiveness of the chemisorption of the adsorbates through analysis of the binding energy of the sulfur atoms. The BE of S $2p_{3/2}$ and S $2p_{1/2}$ have been reported to be ~162 and ~163.2 eV for a sulfur−gold bond and ~163.5 and ~164.7 eV for unbound thiols/disulfides, respectively.[30] Deconvolution of the S 2p peaks is often necessary to determine the extent of bonding for SAMs containing a large amount of unbound sulfur. For this report, the deconvoluted spectra are provided in Figure S3, and the resulting data are provided in Table S2 of the Supporting Information. The XPS spectra show that the SAM formed from **N3PrBnDT** has a greater percentage of bound thiolate on the gold surface than the **N3BnDT** SAM, which shows a large percentage of unbound thiol (or disulfides). In addition, the calculated relative packing densities of the azidoalkanethiolate SAMs reveal that the bidentate adsorbates have reduced packing densities as compared to the monodentate adsorbate (see Table S2 in the Supporting Information), which is in line with reported values in the literature for other bidentate adsorbates.[23,31]

The presence of the azide functional group is apparent in the XPS data. As shown in Figure 2d, peaks at 404 and 401 eV appear in a ratio of 1:2 and represent two distinctly different nitrogen species in the azide group.[17] According to the N 1s and C 1s XPS spectra, the peaks for the **N3BnDT** SAM are shifted ~0.4 eV lower than those of the SAM formed from **N3PrBnDT**. Also, the **N3PrBnDT** SAM exhibits a lower binding energy than that formed from the monothiol, **N3C11SH**. These differences in binding energy can be attributed to the characteristic packing density of the adsorbates on the gold surface. The positive charges that are produced by the loss of photoelectrons discharge more easily in loosely packed SAMs.[32−34] An observed lower binding energy corresponds to a reduction in the packing of the adsorbates in the SAMs, supporting the conclusion that the SAM formed from **N3PrBnDT** packs more densely than that of the SAM formed from **N3BnDT**.

Analysis by PM-IRRAS. To obtain additional information regarding the orientation of the adsorbates on gold for the azide-functionalized SAMs, PM-IRRAS was used to determine the impact of the azide group on the packing of the azide-terminated thin films. Figure 3 shows the PM-IRRAS spectra of

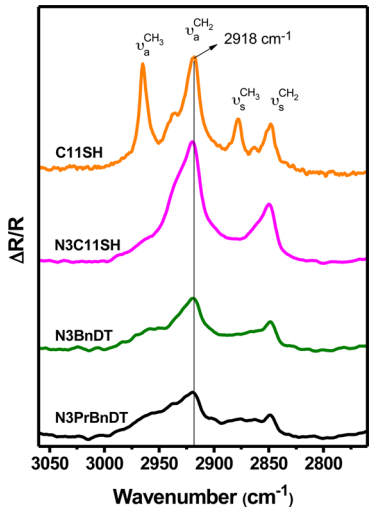

Figure 3. PM-IRRAS spectra of the C−H stretching region for the SAMs generated from **C11SH**, **N3C11SH**, **N3BnDT**, and **N3PrBnDT**.

the normal alkanethiolate and azidoalkanethiolate SAMs for the C−H stretching region. The antisymmetric C−H stretching vibration of the methylene group ($\nu_a^{CH_2}$) was used to make a comparison of the degree of conformational order for the SAMs formed from **C11SH** and **N3C11SH**.[35] The monolayer derived from **C11SH** exhibits a $\nu_a^{CH_2}$ peak at 2918 cm^{-1},

DOI: 10.1021/acs.langmuir.5b00877
Langmuir 2015, 31, 6154−6163

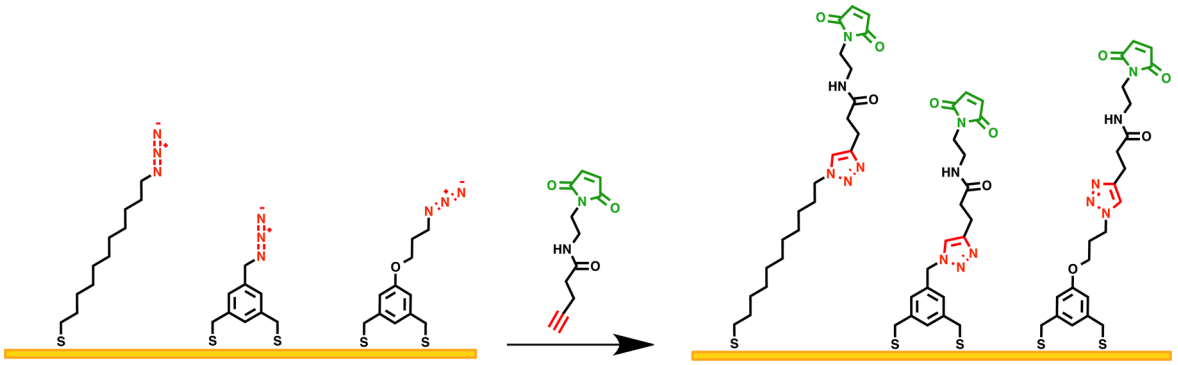

Figure 4. Illustration of the CuAAC click reaction used on the azide-terminated adsorbates for attachment of the maleimide linker to the surface.

indicating a film with alkyl chains that are primarily trans-extended and well-packed, as compared to alkyl chains that are more liquid-like with a $\nu_a^{CH_2}$ peak at ~2926 cm^{-1}.[35,36] The $\nu_a^{CH_2}$ peak for the SAM formed from **N3C11SH** is ~2 cm^{-1} higher as compared to that formed from **C11SH**, which indicates the azide functional group interferes with the packing of the chains of the azidoalkanethiolate SAMs, producing some disorder in the film. Unfortunately, the dithiol adsorbates possess alkyl chain segments in their structures that are too short to allow for the position of the $\nu_a^{CH_2}$ peaks to be used for comparison of the ordering of their SAMs to those of the *n*-alkanethiolate SAM.

Analysis by Contact Angle Goniometry. The use of water as a contacting liquid can provide insight regarding the relative hydrophilicity and packing density of SAMs.[37,38] For the current project, we used contact angle data collected with water as the contacting liquid as a means of comparing the density of the azide groups on our azide-terminated thin films. For the SAM formed from **N3C11SH**, the advancing contact angle of water was 79°, which is consistent with that found in the literature.[17] For the SAM derived from **N3PrBnDT**, the contact angle was 85°, which can be interpreted to indicate that this film had a lower packing density of azide groups on the surface. That is, in a film with a terminal group that is hydrophilic, a higher contact angle might indicate that the underlying methylene groups at the interface are interacting with the contacting liquid.[39,40] This phenomenon appears to be manifest for the dithiol adsorbates in which a propyl chain segment is indirectly attached to the aromatic moiety—a structural arrangement that also produces a different tilt angle for the alkyl chains as compared to a normal alkanethiolate SAM.[24] Because of the hydrophobicity of the alkyl chains, the contact angle value is higher than that for surfaces terminated moreso with azide species.

A macroscopic study by Ong et al. on densely packed SAMs of alkoxy-terminated alkanethiolate adsorbates was used to investigate the depth of penetration of water molecules within the interface of a SAM.[41] These authors used spectroscopic techniques to show that water can intercalate between the alkane chains to a depth of an alkoxy oxygen with a propyl terminus.[41] **N3BnDT** is a short adsorbate with a benzylic azide, and it forms a more loosely packed monolayer than **N3PrBnDT**. For the **N3BnDT** SAM, the advancing contact angle for water was 79°, which is lower than that measured for the **N3PrBnDT** SAM (85°). The lower contact angle for the **N3BnDT** SAM might reflect the reduced packing of the film or the interaction of water molecules with the underlying phenyl groups, which have been shown to be less hydrophobic than alkanethiolate SAMs when presented in an interfacial array.[31]

Addition of the Maleimide Linker to the SAM. *Copper(I)-Catalyzed Click Reaction.* Click attachment of the maleimide linker is the second stage of our stepwise assembly of an array of biomolecules on a flat gold surface. Notably, we chose a maleimide linker rather than connecting poly(L-lysine) directly via propargylglycine because the glycine moiety and the poly(L-lysine) possess amino and carboxylate groups, which can interfere with the CuAAC reaction by inhibiting the copper catalyst and decreasing the yield of the reaction.[42] Additionally, the attached poly(L-lysine) would likely coordinate some of the copper ions, trapping copper salts in the layer, which could potentially decrease the interaction of poly(L-lysine) with other biomolecules and possibly create toxicological concerns when utilizing this peptide array in biological studies. The Cu(I) catalyst was generated by mild reduction of $CuSO_4$ in the presence of sodium ascorbate, activating the reaction between the alkyne functional groups of the maleimide linkers and the azide functional groups on the surface. The click attachment was confirmed by ellipsometry, XPS, PM-IRRAS, and contact angle goniometry.

Analysis by Ellipsometry. For the current set of maleimide-terminated films, the thicknesses of the monolayers increased ~7−10 Å after the CuAAC click reaction illustrated in Figure 4. This increased thickness is less than the estimated length of 13 Å for the maleimide linker chain on the surface. The change in thickness was only 7 Å for the SAM formed from **N3C11SH**, which can be interpreted to reflect a reduction in the density of the newly attached chains due, at least in part, to the inefficiency of this reaction when the azido groups are tightly packed—a concern noted in a prior report.[17] Owing to the lower chain density of the dithiol adsorbates, the observation of a greater increase in the thickness of the SAMs derived from them (10 Å each) demonstrates the efficacy of the malimide linker attachment on these substrates.

Analysis by XPS. Verification that the click reaction was successful is shown in the XPS spectra in Figure 5 for the **N3PrBnDT** SAMs, with the spectra for the **N3C11SH** and **N3BnDT** SAMs provided in the Supporting Information in Figure S4 exhibiting similar results. The region of the XPS spectrum that includes the N 1s BE provides a benchmark for the CuAAC click reaction because the band at ~404 eV (associated with the azide nitrogen)[17] disappears after the click reaction, while a broader band appears at 400 eV. The peak position for the N 1s BE for amide and amine functional groups is also ~400 eV.[17,43] The broadening of the peak in the spectra is attributed to amide groups in different positions and to the presence of a triazole group.[44] The evolution in the N 1s region of the XPS spectrum demonstrates the conversion of the azide

DOI: 10.1021/acs.langmuir.5b00877
Langmuir 2015, 31, 6154−6163

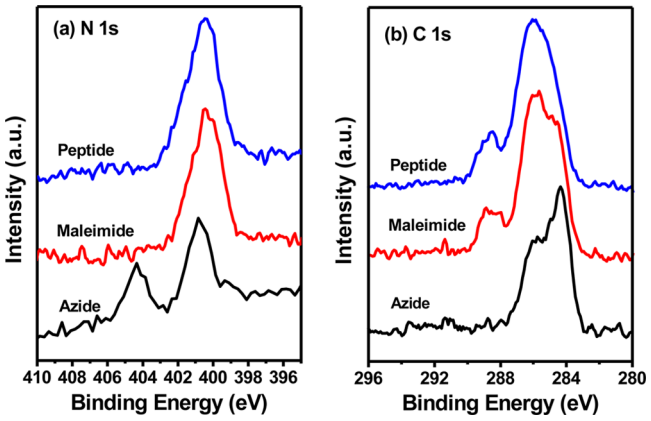

Figure 5. Evolution of the XPS spectra of SAMs derived from **N3PrBnDT** during the stepwise assembly. A change in the spectra appeared in the spectral region (a) for N 1s: a peak at ∼404 eV corresponding to nitrogen with a high oxidation state in the azide group disappears after the click reaction; and (b) for C 1s: for the C−C and C−H binding energies (284−285 eV) and for the C−N and C−O binding energies (286−287 eV), plus a peak appears at a binding energy corresponding to the C═O bonds (∼289 eV) after addition of the maleimide and peptide moieties.

group to a triazole, which confirms the completion of the cycloaddition click reaction. Broadening also occurred in the C 1s band due to the addition of carbon atoms that have slightly different binding energies, particularly in the maleimide moiety; the C═O bond has a C 1s BE of ∼288−289 eV.[27,45] In the C 1s region of the XPS spectrum (Figure 5b), a peak appears at 288.5 eV after the cycloaddition click reaction that corresponds to the amide group in the maleimide linker.

Analysis by PM-IRRAS. The infrared spectrum of an azide-terminated SAM exhibits a peak at ∼2110 cm^{-1}, which is generated by a stretching vibration for the azide moiety.[14] In Figure 6a−c, a loss (or reduction) of the peak at 2105 cm^{-1} in the PM-IRRAS spectra is observed after the attachment of the maleimide linker for all adsorbates, confirming the conversion of the azide functional groups during the click reaction. Note that the spectra in Figure 6c for the SAMs formed from **N3PrBnDT** indicate that the conversion was complete for this substrate. Also, PM-IRRAS analysis of the films after maleimide attachment reveals no alkyne moieties in the film (Figure S5 in the Supporting Information), which is consistent with a model in which there are no maleimide−azide side reactions. In addition, in Figure 6d−f, the presence of the carbonyl groups associated with the maleimide moieties after the click reaction can be verified by changes in the spectra. A band associated with the amide moiety was expected to be observed at ∼1700 cm^{-1} for the maleimide groups on the SAM after the first click reaction.[10] As shown in the spectra, the peak at ∼1720 cm^{-1} corresponds to the maleimide functional group of the attached maleimide linker. These spectra help confirm the successful addition of the linker and provide evidence that the SAM formed from **N3PrBnDT** is a more effective substrate for these attachments.

Analysis by Contact Angle Goniometry. The high sensitivity of water as a contacting liquid for surfaces containing

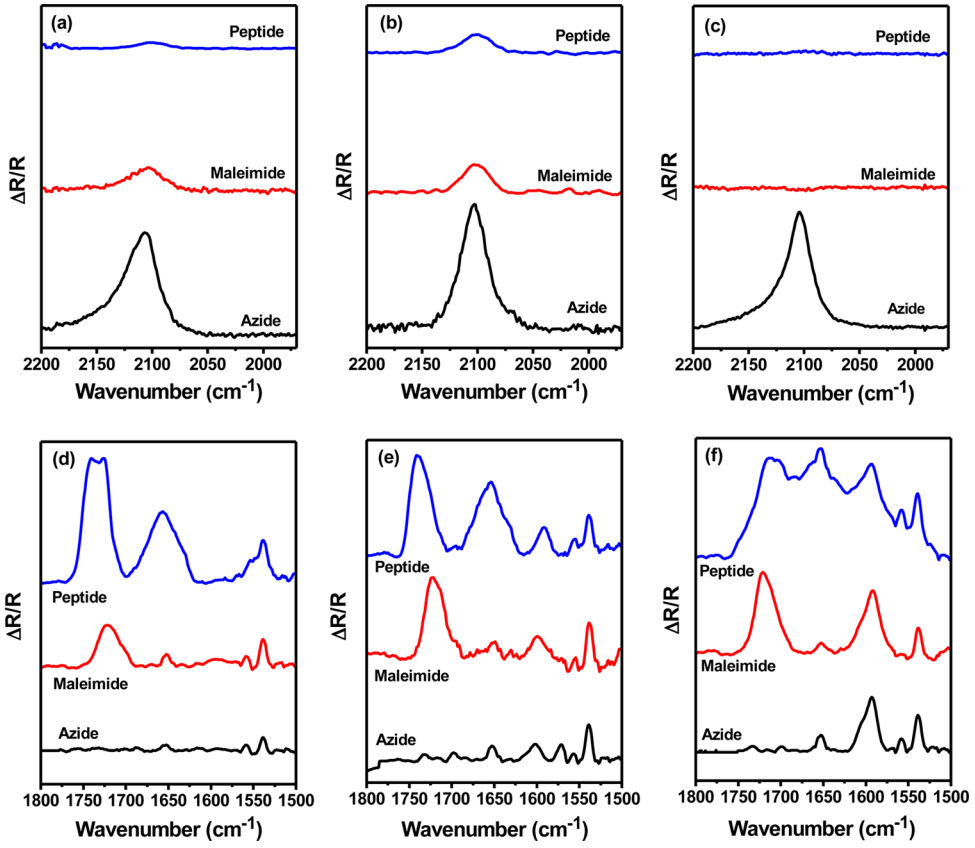

Figure 6. PM-IRRAS spectra of the initial azide-terminated SAMs compared to the modified SAMs for the spectral region associated with an azide stretch for the SAMs formed from (a) **N3C11SH**, (b) **N3BnDT**, and (c) **N3PrBnDT** and for the spectral region associated with carbonyl stretches for the SAMs formed from (d) **N3C11SH**, (e) **N3BnDT**, and (f) **N3PrBnDT**.

DOI: 10.1021/acs.langmuir.5b00877
Langmuir 2015, 31, 6154−6163

heteroatomic groups encouraged us to compare the advancing contact angles for water for the three maleimide-terminated surfaces. The maleimide functional group is a polar group with the potential to engage in hydrogen bonding. The literature indicates that maleimide-modified surfaces with varying film thicknesses exhibit contact angles for water in the range of 41−57°; however, the lower value was observed for a monolayer in which the adsorbates contained an oligoethylene glycol segment.[15,46] In the current study, after the click attachment, the advancing contact angles of water on these surfaces were 44° for the **N3BnDT** SAM, 45° for the **N3C11SH** SAM, and 50° for the **N3PrBnDT** SAM. Considering the values found in the literature,[15,46] these contact angle measurements appear to indicate that the film formed from **N3PrBnDT** more effectively presents an ordered surface array of maleimide moieties than the other two SAMs.

Addition of the Cysteine-Terminated Poly(L-lysine) to the SAM. *Poly(L-lysine) Attachment by Thiol−Michael Addition.* The Michael addition reaction is a well-characterized enolate-type reaction.[19] Here, we used the thiol−Michael addition reaction in buffered conditions to attach a short cysteine-terminated poly(L-lysine) chain onto the SAM-modified gold surfaces. As with the prior steps in our modification of these surfaces, we used a combination of ellipsometry, XPS, PM-IRRAS, and contact angle goniometry to characterize the films and to confirm the presence of lysine at the interface. The peptide used for this study includes five lysine groups, which present positive charges at the surface. The charge repulsion between these peptide moieties plausibly discourages their proximate alignment during attachment to the surface.

Analysis by Ellipsometry. A previous study showed that peptides need sufficient vertical distance from the gold surface to produce effective packing alignments. Thus, attachment on flat gold surfaces demands a barrier or platform SAM;[15] otherwise, the peptides tilt toward the surface, and a well-ordered immobilization cannot be obtained. Such random immobilization of peptides produces a relatively inactive peptide surface.[15,47] Immobilization of peptides has been previously tried on barrier films formed from monodentate thiols.[4,48] Here, we used SAMs formed from both monodentate and bidentate thiols to provide attachment sites on a barrier film with varying packing densities. As shown in Table 1, the thickness of the peptide-modified films increased only ∼3−4 Å after peptide attachment, which likely reflects a low density of attachments to the SAM surface owing to electrostatic repulsions. The incremental changes in thickness in each step are consistent with our XPS elemental analysis (*vide infra*).

Table 1. Ellipsometric Thicknesses for Thin Films Derived from N3C11SH, N3BnDT, and N3PrBnDT Measured after Each Step in the Assembly Process[a]

adsorbate	azide (Å)	maleimide (Å)	peptide (Å)
N3C11SH	11.6 ± 0.5	18.6 ± 1.1	23.4 ± 0.2
N3BnDT	10.0 ± 2.5	19.7 ± 1.1	23.0 ± 0.9
N3PrBnDT	10.6 ± 0.7	20.6 ± 0.6	23.9 ± 1.6

[a]Standard deviations were determined from 12 (azide), 6 (maleimide), and 3 (peptide) data points.

Analysis by XPS. For conducting a compositional analysis, the integrated area under the XPS peaks for key elements can be used to quantify the data.[8,49] For each set of SAMs, the ratio of the area for a specific BE peak can be normalized using the peak area for Au 4f, allowing comparison between SAMs of similar thickness for elements subject to similar levels of attenuation. Figure 7 shows the incremental change in the peak intensity for sulfur, oxygen, and nitrogen on the substrates. As expected, the S/Au ratio increased after peptide attachment owing to the sulfur associated with cysteine; however, the resulting data are skewed by the methods used to compare the adsorbates. The O/Au and N/Au ratios provide an alternative means of comparison and indicate that a more effective poly(L-lysine) attachment occurs on the **N3PrBnDT** SAM.

The high-resolution XPS spectra for **N3PrBnDT** exhibits marked changes in each spectrum of the component elements with each step in the thin-film assembly (see Figure 5). After peptide attachment to the maleimide-terminated **N3PrBnDT** SAM, the shape of the peaks in the C 1s spectrum changed slightly, corresponding to a broader variety of carbon bonds in the poly(L-lysine)-terminated SAM. The peak at 286 eV increased—a BE that is assigned to C−N bonds—and the spectrum also shows an incremental increase at ∼289 eV—a BE that corresponds to an increase in the presence of C═O bonds.[50] In addition, the elemental analysis for nitrogen shows an incremental increase in the N 1s band, which can be attributed to the amine and amide groups in poly(L-lysine). The N 1s spectra also show a broadening in the N 1s band, which might be rationalized by an increase at 400 eV that corresponds to the polypeptide C−N bonds and at ∼402 eV for the protonated amine of lysine.[51] The XPS spectra for the other two peptide-terminated SAMs also reflect these changes (see Figure S4 in the Supporting Information).

Analysis by PM-IRRAS. The PM-IRRAS spectra of the peptide-terminated SAMs formed from azido adsorbates are shown in Figure 6 for the azide and carbonyl regions. Prior reports providing characteristic IR spectra for peptide-modified surfaces show that the amide groups in poly(L-lysine) exhibit vibrational bands in the range of ∼1550−1650 cm^{-1} that vary with the secondary structure of the polypeptide.[52−55] Figure 6 shows a significant increase in intensity for all three SAMs at 1655 cm^{-1}, which indicates the presence of the amide I band of the polypeptide. The weak peak for the amide II band is also present at 1565 cm^{-1} for all three films. The large peak at ∼1750 cm^{-1} corresponds to the stretching vibration of the carbonyl moiety of carboxylic acid (COOH) after poly(L-lysine) attachment to the surface.

The data provided in Figure 6 appear to show a more efficient attachment of the poly(L-lysine) to the **N3PrBnDT** SAM than the other two SAMs. An additional concern we sought to address with this study was whether we could improve the manner in which polypeptides align on a SAM surface. Consequently, we conducted further analysis of this specific SAM for the C−H/O−H/N−H stretching region (see Figure 8). A prior study indicates that the chain segments of the poly(L-lysine) helical structure on top of a thin film could be elucidated by surface IR using certain C−H stretching bands.[56] Therefore, incremental changes in IR intensity in the C−H stretching region after peptide attachment might provide evidence of alignments for the peptide chains. For our SAM, the addition of $\nu_a^{CH_2}$ at 2852 cm^{-1} and $\nu_{as}^{CH_2}$ at 2925 cm^{-1} helps confirm poly(L-lysine) attachment. Additionally, a major peak assigned to poly(L-lysine) at ∼3255 cm^{-1} is a dominant band from the N−H stretching in the amine and amide bonds in the lysine moieties.[56,57]

DOI: 10.1021/acs.langmuir.5b00877
Langmuir 2015, 31, 6154−6163

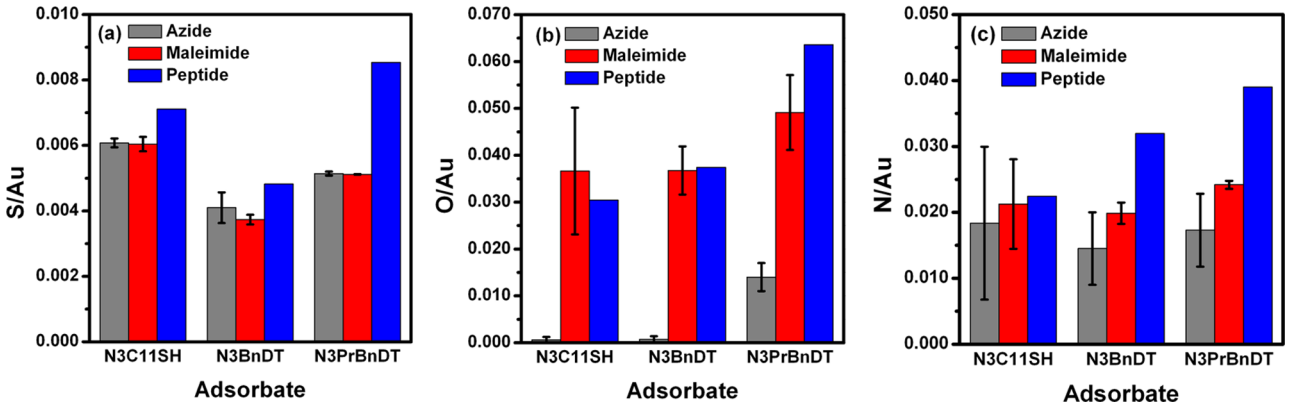

Figure 7. Evolution in sulfur and oxygen peak intensity after stepwise attachments for SAMs initiated with each of the azide-terminated adsorbates. (a) The S/Au ratio for the bidentate adsorbates is divided by two to allow for comparison to the monodentate. (b) The O/Au ratio shows an increase in relative oxygen content for the **N3PrBnDT** SAM after peptide attachment. (c) The N/Au ratio also shows an increase in relative nitrogen content for the **N3PrBnDT** SAM after peptide attachment.

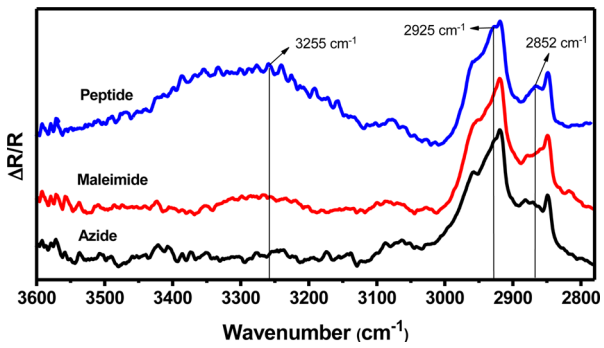

Figure 8. PM-IRRAS spectra of SAMs derived from **N3PrBnDT** show the conversion of the azido-functionalized surface to a lysine-coated surface. Specific vibrations for the lysine groups are indicated in the figure: the $\nu_a^{CH_2}$ at 2852 cm^{-1}, the $\nu_{as}^{CH_2}$ at 2925 cm^{-1}, and the N−H stretching vibration at 3255 cm^{-1} associated with the amine and amide bonds.[56]

Analysis by Contact Angle Goniometry. Advancing contact angle data were collected for the fully assembled SAMs using water as the contacting liquid with the following results: **N3C11SH** SAM, 31°; **N3BnDT** SAM, 32°; and **N3PrBnDT** SAM, 41°. The contact angle for each of the monolayers decreased ∼11−14° after poly(L-lysine) attachment to the maleimide-modified surfaces (see Table S3 in the Supporting Information). For this particular peptide-modified interface, reference data are limited; however, SAMs formed by the physisorption of poly(L-lysine) produced surfaces with contact angles ranging from 42° to 52°,[58] which is consistent with the values observed for the **N3PrBnDT** SAM. In addition, it is worth noting that at each stage of the assembly the SAM formed from **N3PrBnDT** consistently produced higher contact angle values than the other two SAMs.

Mixed Alkanethiolate SAMs vs Single-Component Dithiolate SAMs. Because of the prevalence of the use of mixed SAMs for diluting the presence of reactive sites on a substrate, a number of mixed-SAM studies have involved azidothiolates.[14,17] Their application in click chemistry research has focused primarily on improving the efficiency of the click attachment reaction by diluting the presence of the azide moiety at the SAM interface. However, the preparation of homogeneous mixed SAMs from a deposition solution with a predetermined percentage of azidoalkanethiol remains challenging. Similar problems were explored in a prior mixed-SAM study by our group using partially fluorinated alkanethiols and a normal alkanethiol.[49] This project demonstrated how diverse adsorbates can lead to surface compositions in the developed SAMs that are markedly different from the composition of the adsorbates in solution. A variety of factors contribute to such disparities, including solvent−adsorbate interactions and adsorbate steric bulk.[8,59]

For the current system, a series of mixed SAMs formed from **C11SH** and **N3C11SH** were pursued. The solvents tested for mixed-SAM development were isooctane (nonpolar) and DMSO (polar). A comparison of the initial data for the SAMs formed from these two solvents led to the decision to use DMSO for the mixed SAMs described in this report (see Figure S6, Table S4, and the corresponding discussion in the Supporting Information for further details). Data obtained by XPS was used to develop N/Au ratios for the mixed SAMs to investigate the relative presence of the azido adsorbate on the surface as compared to that of **N3C11SH** in solution for deposition solutions containing 0.2, 0.4, 0.5, 0.6, and 0.8 mole fraction **N3C11SH**. Figure 9a shows the data for the mixed-SAM series, revealing that the mole fraction of azidoalkanethiol on the gold surface is lower than that in the solution phase, reflecting a preference for **N3C11SH** in the DMSO solution phase over **C11SH**.

XPS analysis can also be used to determine the efficiency of the click cycloaddition reaction on the azide-functionalized surfaces. To accomplish this task, we used the mole fraction of **N3C11SH** on the surface in the mixed SAMs series in a comparison with the bidentate aromatic adsorbates after the initial click reaction. For our calculations, the mole fraction of maleimide-modified **N3C11SH** on the surface was used to determine the yield of the click cycloaddition reaction using an assumption that the pure **N3C11SH** SAM represented 100% conversion. Additionally, all data were normalized using the data for that SAM. Previous studies working with azidoalkanethiolate SAMs showed that the coverage for the clicked attachment of molecules on the surface was about 55% due to steric limitations from secondary molecules, but this percentage is dependent upon the specific molecule being attached.[17] The click reaction for our mixed SAMs was monitored by XPS to study the C 1s region of the spectrum, more specifically the C═O bonds of maleimide. The ratio of C═O/Au was used to

DOI: 10.1021/acs.langmuir.5b00877
Langmuir 2015, 31, 6154−6163

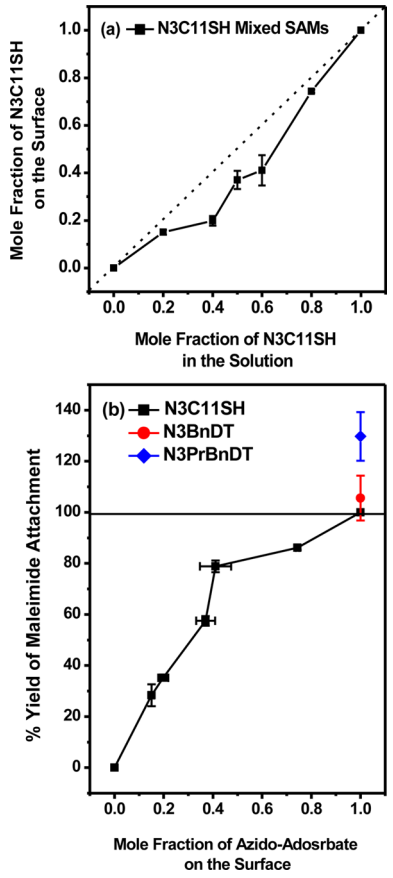

Figure 9. Surface composition analysis developed from XPS data: (a) for the mole fraction of azide adsorbates on the surface versus the mole fraction in solution for mixed SAMs developed in DMSO and (b) for the percent yield attachment of maleimide on the mixed SAMs developed in DMSO using an assumption of 100% conversion for the pure **N3C11SH** SAM, while also normalizing the data to that SAM. Included in (b) are the data for the bidentate SAMs.

make our comparisons. Detailed calculations are presented in Table S5 of the Supporting Information.

As shown in the PM-IRRAS spectra in Figure 6, some of the nonreacted azide functional groups remain on the surface after completion of the click reaction for the SAMs formed from **N3C11SH** and **N3BnDT**; therefore maleimide attachment is incomplete for those SAMs. In Figure 9b, the coverage of maleimide in our mixed SAMs exhibits a trend that is consistent with the literature; a decrease in the fraction of azide functional groups on the surface is associated with an increase in the efficiency of the click attachments.[17] The maleimide surface coverage for the SAM formed from **N3PrBnDT** is 130% of that of **N3C11SH**, while that of the **N3BnDT** SAM is roughly the same as the **N3C11SH** SAM. Despite the lower packing density of the SAMs generated from **N3PrBnDT** as compared to the series of mixed azidoalkanthiolate SAMs (see Table S2 in the Supporting Information), **N3PrBnDT** SAMs have better coverage of maleimide on the surface. These results confirm our conclusion that the azido click reaction can be more efficient using our custom-designed aromatic dithiol adsorbates. We believe that the improvement reflects a reduction in steric hindrance for the less densely packed aromatic dithiol adsorbates having a short alkyl spacer.

CONCLUSIONS

Azide-terminated adsorbates were synthesized and successfully self-assembled on the surface of gold to form a platform for the CuAAC click reaction attachment of an alkyne-terminated maleimide linker, followed by a second click reaction to attach a thiol-terminated poly(L-lysine) chain with five lysine residues. These SAMs were formed from a monodentate azidoalkanethiol and two short azide-terminated aromatic bidentate adsorbates and were compared against an alkanethiolate reference SAM. Quantitative and qualitative analyses of the data collected by ellipsometry and XPS show that the bidentate adsorbates possessing an aromatic moiety produce films of suitable packing density for successful click reactions, which is attributed to the absence of steric hindrance for the azide group in these less densely packed films. This conclusion was verified with a series of mixed SAMs formed from the monodentate azidoalkanethiol and a normal alkanethiol, where none of the mixed films yielded coverage of maleimide as effectively as the SAM formed from **N3PrBnDT**. PM-IRRAS data indicate that the reaction for the maleimide attachment was incomplete for the SAMs formed from **N3C11SH** and **N3BnDT**, while the spectrum for the **N3PrBnDT** SAM shows no indication of any residual azide. Additionally, contact angle data using water as a contacting liquid show that **N3PrBnDT** generates films that present the attached large molecules more effectively than the SAM formed from **N3BnDT**. From these results, we conclude that SAMs formed from **N3PrBnDT** provide a suitable and stable platform for attachment of secondary molecules, producing well-ordered molecular arrays on a gold surface and avoiding the complications associated with preparing mixed-adsorbate films. Future studies involving this new adsorbate system will provide for the attachment of large molecules to gold nanoparticles for drug-delivery applications.

ASSOCIATED CONTENT

Supporting Information

Synthetic procedures are provided for **N3BnDT**, **N3PrBnDT**, and the maleimide linker, along with their ^{1}H and ^{13}C NMR spectra; analysis of solvent tests for developing SAMs, instrumental procedures, deconvoluted XPS spectra, packing density data, detailed contact angle data, supplemental PM-IRRAS spectra, and additional XPS spectra and elemental analyses (Figures S1−S12, Schemes S1−S3, and Tables S1−S5). The Supporting Information is available free of charge on the ACS Publications website at DOI: 10.1021/acs.langmuir.5b00877.

AUTHOR INFORMATION

Corresponding Author

*E-mail: trlee@uh.edu (T.R.L.).

Notes

The authors declare no competing financial interest.

ACKNOWLEDGMENTS

We thank the Robert A. Welch Foundation (E-1320) and the Texas Center for Superconductivity for supporting this research. Additional funding for this project was provided by the Chemical Biology Interdisciplinary Program (CBIP) at the University of Houston.

DOI: 10.1021/acs.langmuir.5b00877
Langmuir 2015, 31, 6154−6163

REFERENCES

(1) Akkahat, P.; Mekboonsonglarp, W.; Kiatkamjornwong, S.; Hoven, V. P. Surface-Grafted Poly(acrylic acid) Brushes as a Precursor Layer for Biosensing Applications: Effect of Graft Density and Swellability on the Detection Efficiency. *Langmuir* **2012**, *28*, 5302−5311.

(2) Rusmini, F.; Zhong, Z.; Feijen, J. Protein Immobilization Strategies for Protein Biochips. *Biomacromolecules* **2007**, *8*, 1775−1789.

(3) Dalsin, J. L.; Hu, B.-H.; Lee, B. P.; Messersmith, P. B. Mussel Adhesive Protein Mimetic Polymers for the Preparation of Nonfouling Surfaces. *J. Am. Chem. Soc.* **2003**, *125*, 4253−4258.

(4) Acevedo-Vélez, C.; Andre, G.; Dufrêne, Y. F.; Gellman, S. H.; Abbott, N. L. Single-Molecule Force Spectroscopy of β-Peptides That Display Well-Defined Three-Dimensional Chemical Patterns. *J. Am. Chem. Soc.* **2011**, *133*, 3981−3988.

(5) Ivanov, I. E.; Morrison, A. E.; Cobb, J. E.; Fahey, C. A.; Camesano, T. A. Creating Antibacterial Surfaces with the Peptide Chrysophsin-1. *ACS Appl. Mater. Interfaces* **2012**, *4*, 5891−5897.

(6) Wang, Z.; Han, X.; He, N.; Chen, Z.; Brooks, C. L. Environmental Effect on Surface Immobilized Biological Molecules. *J. Phys. Chem. B* **2014**, *118*, 12176−12185.

(7) Han, X. F.; Liu, Y. W.; Wu, F. G.; Jansensky, J.; Kim, T.; Wang, Z. L.; Brooks, C. L.; Wu, J. F.; Xi, C. W.; Mello, C. M.; Chen, Z. Different interfacial behaviors of peptides chemically immobilized on surfaces with different linker lengths and via different termini. *J. Phys. Chem. B* **2014**, *118*, 2904−2912.

(8) Bain, C. D.; Evall, J.; Whitesides, G. M. Formation of Monolayers by the Coadsorption of Thiols on Gold: Variation in the Head Group, Tail Group, and Solvent. *J. Am. Chem. Soc.* **1989**, *111*, 7155−7164.

(9) Lee, J. K.; Lee, K.-B.; Kim, D. J.; Choi, I. S. Reactivity of Vinyl-Terminated Self-Assembled Monolayers on Gold: Olefin Cross-Metathesis Reactions. *Langmuir* **2003**, *19*, 8141−8143.

(10) Smith, E. A.; Wanat, M. J.; Cheng, Y.; Barreira, S. V. P.; Frutos, A. G.; Corn, R. M. Formation, Spectroscopic Characterization, and Application of Sulfhydryl-Terminated Alkanethiol Monolayers for the Chemical Attachment of DNA onto Gold Surfaces. *Langmuir* **2001**, *17*, 2502−2507.

(11) Baas, T.; Gamble, L.; Hauch, K. D.; Castner, D. G.; Sasaki, T. Characterization of a Cysteine-Containing Peptide Tether Immobilized onto a Gold Surface. *Langmuir* **2002**, *18*, 4898−4902.

(12) Liu, Y.; Ogorzalek, T. L.; Yang, P.; Schroeder, M. M.; Marsh, E. N. G.; Chen, Z. Molecular Orientation of Enzymes Attached to Surfaces through Defined Chemical Linkages at the Solid−Liquid Interface. *J. Am. Chem. Soc.* **2013**, *135*, 12660−12669.

(13) Ye, S.; Nguyen, K. T.; Boughton, A. P.; Mello, C. M.; Chen, Z. Orientation Difference of Chemically Immobilized and Physically Adsorbed Biological Molecules on Polymers Detected at the Solid/Liquid Interfaces in Situ. *Langmuir* **2009**, *26*, 6471−6477.

(14) Hudalla, G. A.; Murphy, W. L. Using "Click" Chemistry to Prepare SAM Substrates to Study Stem Cell Adhesion. *Langmuir* **2009**, *25*, 5737−5746.

(15) Wetterö, J.; Hellerstedt, T.; Nygren, P.; Broo, K.; Aili, D.; Liedberg, B.; Magnusson, K.-E. Immobilized Chemoattractant Peptides Mediate Adhesion and Distinct Calcium-Dependent Cell Signaling in Human Neutrophils. *Langmuir* **2008**, *24*, 6803−6811.

(16) Furst, A. L.; Hill, M. G.; Barton, J. K. DNA-Modified Electrodes Fabricated Using Copper-Free Click Chemistry for Enhanced Protein Detection. *Langmuir* **2013**, *29*, 16141−16149.

(17) Collman, J. P.; Devaraj, N. K.; Eberspacher, T. P. A.; Chidsey, C. E. D. Mixed Azide-Terminated Monolayers: A Platform for Modifying Electrode Surfaces. *Langmuir* **2006**, *22*, 2457−2464.

(18) Santos, C. M.; Kumar, A.; Kolar, S. S.; Contreras-Caceres, R.; McDermott, A.; Cai, C. Immobilization of Antimicrobial Peptide IG-25 onto Fluoropolymers via Fluorous Interactions and Click Chemistry. *ACS Appl. Mater. Interfaces* **2013**, *5*, 12789−12793.

(19) Nair, D. P.; Podgórski, M.; Chatani, S.; Gong, T.; Xi, W.; Fenoli, C. R.; Bowman, C. N. The Thiol-Michael Addition Click Reaction: A Powerful and Widely Used Tool in Materials Chemistry. *Chem. Mater.* **2014**, *26*, 724−744.

(20) Son, S. J.; Lee, S. B. Controlled Gold Nanoparticle Diffusion in Nanotubes: Platfom of Partial Functionalization and Gold Capping. *J. Am. Chem. Soc.* **2006**, *128*, 15974−15975.

(21) Sano, K.-I.; Shiba, K. A Hexapeptide Motif that Electrostatically Binds to the Surface of Titanium. *J. Am. Chem. Soc.* **2003**, *125*, 14234−14235.

(22) Garg, N.; Carrasquillo-Molina, E.; Lee, T. R. Self-Assembled Monolayers Composed of Aromatic Thiols on Gold: Structural Characterization and Thermal Stability in Solution. *Langmuir* **2002**, *18*, 2717−2726.

(23) Lee, H. J.; Jamison, A. C.; Yuan, Y.; Li, C.-H.; Rittikulsittichai, S.; Rusakova, I.; Lee, T. R. Robust Carboxylic Acid-Terminated Organic Thin Films and Nanoparticle Protectants Generated from Bidentate Alkanethiols. *Langmuir* **2013**, *29*, 10432−10439.

(24) Garg, N.; Lee, T. R. Self-Assembled Monolayers Based on Chelating Aromatic Dithiols on Gold. *Langmuir* **1998**, *14*, 3815−3819.

(25) Miura, Y. F.; Takenaga, M.; Koini, T.; Graupe, M.; Garg, N.; Graham, R. L.; Lee, T. R. Wettabilities of Self-Assembled Monolayers Generated from CF_3-Terminated Alkanethiols on Gold. *Langmuir* **1998**, *14*, 5821−5825.

(26) Bruno, G.; Babudri, F.; Operamolla, A.; Bianco, G. V.; Losurdo, M.; Giangregorio, M. M.; Hassan Omar, O.; Mavelli, F.; Farinola, G. M.; Capezzuto, P.; Naso, F. Tailoring Density and Optical and Thermal Behavior of Gold Surfaces and Nanoparticles Exploiting Aromatic Dithiols. *Langmuir* **2010**, *26*, 8430−8440.

(27) Tam-Chang, S.-W.; Biebuyck, H. A.; Whitesides, G. M.; Jeon, N.; Nuzzo, R. G. Self-Assembled Monolayers on Gold Generated from Alkanethiols with the Structure $RNHCOCH_2SH$. *Langmuir* **1995**, *11*, 4371−4382.

(28) Mattiuzzi, A.; Jabin, I.; Mangeney, C.; Roux, C.; Reinaud, O.; Santos, L.; Bergamini, J.-F.; Hapiot, P.; Lagrost, C. Electrografting of Calix[4]arenediazonium Salts To Form Versatile Robust Platforms for Spatially Controlled Surface Functionalization. *Nat. Commun.* **2012**, *3*, 1130−1137.

(29) Heinrich, T.; Traulsen, C. H. H.; Darlatt, E.; Richter, S.; Poppenberg, J.; Traulsen, N. L.; Linder, I.; Lippitz, A.; Dietrich, P. M.; Dib, B.; Unger, W. E. S.; Schalley, C. A. The Versatility of "Click" Reactions: Molecular Recognition at Interfaces. *RSC Adv.* **2014**, *4*, 17694−17702.

(30) Yang, Y. W.; Fan, L. J. High-Resolution XPS Study of Decanethiol on Au(111): Single Sulfur−Gold Bonding Interaction. *Langmuir* **2002**, *18*, 1157−1164.

(31) Shon, Y.-S.; Colorado, R.; Williams, C. T.; Bain, C. D.; Lee, T. R. Low-Density Self-Assembled Monolayers on Gold Derived from Chelating 2-Monoalkylpropane-1,3-dithiols. *Langmuir* **1999**, *16*, 541−548.

(32) Ishida, T.; Hara, M.; Kojima, I.; Tsuneda, S.; Nishida, N.; Sasabe, H.; Knoll, W. High Resolution X-ray Photoelectron Spectroscopy Measurements of Octadecanethiol Self-Assembled Monolayers on Au(111). *Langmuir* **1998**, *14*, 2092−2096.

(33) Kaindl, G.; Chiang, T. C.; Eastman, D. E.; Himpsel, F. J. Distance-Dependent Relaxation Shifts of Photoemission and Auger Energies for Xe on Pd(001). *Phys. Rev. Lett.* **1980**, *45*, 1808−1811.

(34) Park, J.-S.; Vo, A. N.; Barriet, D.; Shon, Y.-S.; Lee, T. R. Systematic Control of the Packing Density of Self-Assembled Monolayers Using Bidentate and Tridentate Chelating Alkanethiols. *Langmuir* **2005**, *21*, 2902−2911.

(35) Porter, M. D.; Bright, T. B.; Allara, D. L.; Chidsey, C. E. D. Spontaneously Organized Molecular Assemblies. 4. Structural Characterization of n-alkyl Thiol Monolayers on Gold by Optical Ellipsometry, Infrared Spectroscopy, and Electrochemistry. *J. Am. Chem. Soc.* **1987**, *109*, 3559−3568.

(36) Bensebaa, F.; Voicu, R.; Huron, L.; Ellis, T. H.; Kruus, E. Kinetics of Formation of Long-Chain n-Alkanethiolate Monolayers on Polycrystalline Gold. *Langmuir* **1997**, *13*, 5335−5340.

(37) Morra, M.; Occhiello, E.; Garbassi, F. Knowledge about Polymer Surfaces from Contact Angle Measurements. *Adv. Colloid Interface Sci.* **1990**, *32*, 79−116.

DOI: 10.1021/acs.langmuir.5b00877
Langmuir 2015, 31, 6154−6163

(38) Graupe, M.; Takenaga, M.; Koini, T.; Colorado, R.; Lee, T. R. Oriented Surface Dipoles Strongly Influence Interfacial Wettabilities. *J. Am. Chem. Soc.* **1999**, *121*, 3222−3223.
(39) Wilson, M. D.; Ferguson, G. S.; Whitesides, G. M. Size of Alkyl Group R: Principal Factor Determining Wettability of Surface-Functionalized Polyethylenes (PE-CONHR and PE-CO_2R) by Water. *J. Am. Chem. Soc.* **1990**, *112*, 1244−1245.
(40) Béthencourt, M. I.; Srisombat, L.-o.; Chinwangso, P.; Lee, T. R. SAMs on Gold Derived from the Direct Adsorption of Alkanethioacetates Are Inferior to Those Derived from the Direct Adsorption of Alkanethiols. *Langmuir* **2009**, *25*, 1265−1271.
(41) Ong, T. H.; Davies, P. B.; Bain, C. D. Sum-Frequency Spectroscopy of Monolayers of Alkoxy-Terminated Alkanethiols in Contact with Liquids. *Langmuir* **1993**, *9*, 1836−1845.
(42) Ahmad Fuaad, A. A. H.; Azmi, F.; Skwarczynski, M.; Toth, I. Peptide Conjugation via CuAAC 'Click' Chemistry. *Molecules* **2013**, *18*, 13148−13174.
(43) Gouget-Laemmel, A. C.; Yang, J.; Lodhi, M. A.; Siriwardena, A.; Aureau, D.; Boukherroub, R.; Chazalviel, J. N.; Ozanam, F.; Szunerits, S. Functionalization of Azide-Terminated Silicon Surfaces with Glycans Using Click Chemistry: XPS and FTIR Study. *J. Phys. Chem. C* **2013**, *117*, 368−375.
(44) Chelmowski, R.; Käfer, D.; Köster, S. D.; Klasen, T.; Winkler, T.; Terfort, A.; Metzler-Nolte, N.; Wöll, C. Postformation Modification of SAMs: Using Click Chemistry to Functionalize Organic Surfaces. *Langmuir* **2009**, *25*, 11480−11485.
(45) Böcking, T.; James, M.; Coster, H. G. L.; Chilcott, T. C.; Barrow, K. D. Structural Characterization of Organic Multilayers on Silicon(111) Formed by Immobilization of Molecular Films on Functionalized Si−C Linked Monolayers. *Langmuir* **2004**, *20*, 9227−9235.
(46) Seto, H.; Takara, M.; Yamashita, C.; Murakami, T.; Hasegawa, T.; Hoshino, Y.; Miura, Y. Surface Modification of Siliceous Materials Using Maleimidation and Various Functional Polymers Synthesized by Reversible Addition−Fragmentation Chain Transfer Polymerization. *ACS Appl. Mater. Interfaces* **2012**, *4*, 5125−5133.
(47) Gitelman, A.; Rapaport, H. Bifunctional Designed Peptides Induce Mineralization and Binding to TiO_2. *Langmuir* **2014**, *30*, 4716−4724.
(48) Trzcinska, R.; Balin, K.; Kubacki, J.; Marzec, M. E.; Pedrys, R.; Szade, J.; Silberring, J.; Dworak, A.; Trzebicka, B. Relevance of the Poly(ethylene glycol) Linkers in Peptide Surfaces for Proteases Assays. *Langmuir* **2014**, *30*, 5015−5025.
(49) Jamison, A. C.; Zhang, S.; Zenasni, O.; Schwartz, D. K.; Lee, T. R. Fibrillar Self-Organization of a Line-Active Partially Fluorinated Thiol within Binary Self-Assembled Monolayers. *Langmuir* **2012**, *28*, 16834−16844.
(50) Xu, L. Q.; Jiang, H.; Neoh, K.-G.; Kang, E.-T.; Fu, G. D. Poly(dopamine acrylamide)-co-poly(propargyl acrylamide)-Modified Titanium Surfaces for 'Click' Functionalization. *Polym. Chem.* **2012**, *3*, 920−927.
(51) Yam, C.-M.; Zheng, L.; Salmain, M.; Pradier, C.-M.; Marcus, P.; Jaouen, G. Labelling and Binding of Poly-(L-lysine) to Functionalized Gold Surfaces. Combined FT-IRRAS and XPS Characterization. *Colloids Surf., B* **2001**, *21*, 317−327.
(52) Li, N.; Zhang, X.; Wang, Q.; Wang, F.; Shen, P. Biomimetic Synthesis of Silica Hollow Spheres Using Poly (l-lysine) and Mechanism Research. *RSC Adv.* **2012**, *2*, 3288−3297.
(53) Müller, M. Orientation of α-Helical Poly(l-lysine) in Consecutively Adsorbed Polyelectrolyte Multilayers on Texturized Silicon Substrates. *Biomacromolecules* **2001**, *2*, 262−269.
(54) Rozenberg, M.; Shoham, G. FTIR Spectra of Solid Poly-l-lysine in the Stretching NH Mode Range. *Biophys. Chem.* **2007**, *125*, 166−171.
(55) York, R. L.; Holinga, G. J.; Somorjai, G. A. An Investigation of the Influence of Chain Length on the Interfacial Ordering of l-Lysine and l-Proline and Their Homopeptides at Hydrophobic and Hydrophilic Interfaces Studied by Sum Frequency Generation and Quartz Crystal Microbalance. *Langmuir* **2009**, *25*, 9369−9374.
(56) Jordon, C. E.; Frey, B. L.; Kornguth, S.; Corn, R. M. Characterization of Poly-L-lysine Adsorption onto Alkanethiol-Modified Gold Surfaces with Polarization-Modulation Fourier Transform Infrared Spectroscopy and Surface Plasmon Resonance Measurements. *Langmuir* **1994**, *10*, 3642−3648.
(57) Keller, T. F.; Müller, M.; Ouyang, W.; Zhang, J.-T.; Jandt, K. D. Templating α-Helical Poly(l-lysine)/Polyanion Complexes by Nanostructured Uniaxially Oriented Ultrathin Polyethylene Films. *Langmuir* **2010**, *26*, 18893−18901.
(58) Yamanlar, S.; Sant, S.; Boudou, T.; Picart, C.; Khademhosseini, A. Surface Functionalization of Hyaluronic acid Hydrogels by Polyelectrolyte Multilayer Films. *Biomaterials* **2011**, *32*, 5590−5599.
(59) Bain, C. D.; Whitesides, G. M. Formation of Monolayers by the Coadsorption of Thiols on Gold: Variation in the Length of the Alkyl Chain. *J. Am. Chem. Soc.* **1989**, *111*, 7164−7175.

DOI: 10.1021/acs.langmuir.5b00877
Langmuir 2015, 31, 6154−6163